Time-dependent receiver extension for FWI: a dynamic programming approach

M. Benziane[1], R. Brossier[1], L. Métivier[1,2]

[1] Univ. Grenoble Alpes ISTerre; [2] Univ. Grenoble Alpes CNRS LJK

Summary

Extension strategies rely on introducing additional degrees of freedom to FWI, extending the search space. Extension strategies circumvent cycle-skipping by fitting the observed and calculated data when the model estimate is poor. Time-dependent receiver extension introduces the receiver position as a free parameter, allowing it to move as a function of the acquisition time, which permits to obtain a fit in a wrong velocity model. In previous works, we have proposed to parameterize the time-dependent receiver extension using a polynomial interpolation, to reduce the computational complexity of the approach, obtaining the optimal values at specified control points using stochastic optimization. This still can cause limitations: in specific cases, complex relocalization could be needed, which would lead to large number of control points, making the strategy computationally intractable. This is the motivation of the present study, where we replace this parametrization and stochastic optimization with an all-in-one dynamic programming approach. This is possible thanks to the analogy between Dynamic Time Warping of seismic images and our time-dependent receiver extension. Numerical experiments in 2D show how the dynamic programming approach reduces the computational cost, while maintaining a finer discretization, and relying on a deterministic optimization process.

Time-dependent receiver extension for FWI: a dynamic programming approach

Introduction

Full Waveform Inversion (FWI) has become the academia and the industry standard for high resolution seismic imaging. It is formulated as a PDE constrained optimization problem, where the fit between the observed and synthetic data is improved, by iteratively updating a given initial model. However, when the initial model is not accurate, causing a phase mismatch of more than half the dominant period between the observed and calculated data, FWI converges to a non-informative solution, matching the wrong phases with each other (Virieux and Operto, 2009). This phase ambiguity is the well known cycle-skipping issue. Numerous strategies have been developed to overcome this issue, the review of which is beyond the scope of this study. Our work focuses on a class of methods which relies on introducing additional degrees of freedom to the FWI problem. This search space extension circumvents cycle-skipping by fitting the data when the model estimate is poor. In this study, we focus on receiver position extension (Métivier and Brossier, 2022). Receiver extension introduces the receiver position as a free parameter. The resulting problem is a two nested-loops optimization, where the outer loop is the conventional FWI optimization loop, which updates the model mechanical parameters. The inner loop solves the subproblem of finding the optimal receivers relocalizations which explain the data better. We have extended the method by making the receiver relocalization time-dependent, in order to account for multiple arrivals (Benziane et al., 2024). We achieve this by using a piecewise polynomial temporal parametrization. The receiver relocalization is thus obtained from a set of control points using interpolating polynomials. The optimal relocalization values at the control points are obtained using a stochastic optimization strategy. While we have noted that this approach is efficient on 2D and 3D realistic synthetic case studies, it can still become computationally expensive when complex relocalization profiles are required to handle complex multi-arrival data. In this case, the increase in the number of control points leads to an unaffordable computational cost for the inner loop. Also, the use of stochastic optimization requires specific tuning which can be difficult to set, and by essence it is not guaranteed to fully be able to reproduce the same results upon multiple FWIs. For this reason, we are interested in exploring an alternative deterministic approach, which does not rely on such a polynomial interpolation. Based on an analogy with our time-dependent receiver relocalization and the Dynamic Time Warping proposed by Ma and Hale (2013) and Hale (2013), we explore the feasibility of using a dynamic programming approach to solve the inner loop of our extension strategy.

Time-dependent receiver extension for FWI

We write the receiver-extension minimization problem as

$$\min_{m,\Delta x(t)} f(m,\Delta x(t)) \triangleq \min_{m,\Delta x(t)} \frac{1}{2}\sum_{s=1}^{N_s}\sum_{r=1}^{N_r}\int |d_{cal,s}(\mathbf{x}_r+\Delta x_{s,r}(t),t)-d_{obs,s}(\mathbf{x}_r,t)|^2 dt + \alpha \mathscr{P}_1[\Delta x_{s,r}(t)] + \beta \mathscr{P}_2[\Delta \dot{x}_{s,r}(t)(t)], \tag{1}$$

where $d_{cal,s}(x_r+\Delta x_{s,r}(t),t)]$ are the extended calculated data, which are extracted from the synthetic wavefield, that is computed using a wave equation. $d_{obs,s}(\mathbf{x}_r,t)$ are the observed data, the subscripts s and r are the source and receiver indices, respectively, N_s is the total number of sources, and N_r is the total number of receivers. The quantity $\Delta x_{s,r}(t)$ is the time-dependent receiver relocalization, that is, a spatial shift of a receiver r which depends on the acquisition time. The second term in the right hand side ($\mathscr{P}_1$) is a penalty term, which controls the receiver position so it is not too large, and forces it to zero as the model estimate improves, with α being a tuning parameter. Similarly, the third term in the right hand side ($\mathscr{P}_2$) is a penalty term which constrains the receiver speed, with β being a tuning parameter. The second penalty term is needed to mitigate the frequency content changes, which occur when a receiver moves as a function of time. These frequency content changes are attributed to Doppler effect. Our bi-variate misfit function is minimized using a nested loops strategy. The outer loop is the conventional FWI loop, which updates the model parameters m for a an optimal relocalization $\overline{\Delta x_{s,r}(t)}$. The inner loop obtains the optimal receiver relocalization $\overline{\Delta x_{s,r}(t)}$ for a fixed m. In our previous work (Benziane et al., 2024), we use a piecewise polynomial interpolation to parametrize the time-dependent relocalization $\Delta x_{s,r}(t)$. The time vector is divided into segments, each of which contains a Lagrange polynomial. The time-dependent relocalization is thus defined as follows

$$\Delta x(t) = \sum_{j=1}^{n_s}\sum_{k=1}^{N_\ell} a_{k+N_\ell\times(j-1)}\ell_k^{N_\ell}(t), \tag{2}$$

where $\ell_k^{N_\ell}(t)$ are Lagrange basis functions of order N_ℓ, n_s is the number of segments and a_i ($i=k+N_\ell\times(j-1)$) are the values at the control points.

In the inner loop we aim at finding the optimal a_i values, that define the time-dependent virtual receivers positions. The unknowns for this subproblem are therefore $a = (a_1, a_2, .., a_{N_\ell \times n_s + 1})^T$. We rewrite the minimization of equation 1

$$\min_{m,a} f(m,a). \tag{3}$$

The optimal a is obtained using a global optimization strategy. In our previous work, we have used Particle Swarm Optimization (PSO) (Kennedy and Eberhart, 1995).

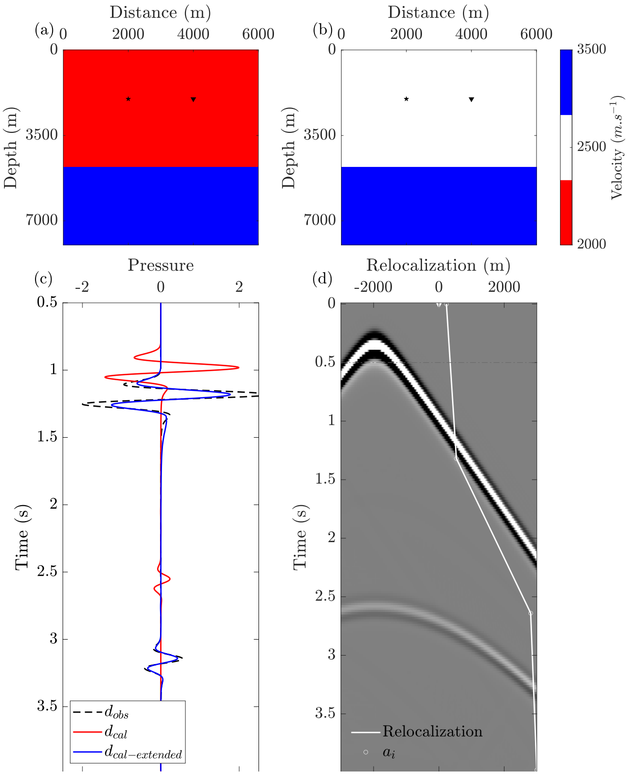

Figure 1: *Time-dependent receiver extension illustration. (a): True velocity model. (b): Initial velocity model. (c): Data fit, observed trace shown in a dashed black line, synthetic trace in a red solid line and the extended trace in a blue solid line. (d): Extended trace extraction from the synthetic wavefield shown in gray scale, the relocalization time profile is shown in a white solid line.*

We explain the time-dependent relocalization strategy using a simple numerical experiment (Figure 1). Consider one layer with $v_p = 2000$ m.s^{-1} over a half-space with $v_p = 3500$ m.s^{-1}. We generate the observed data in this model, we show a single trace of the observed data in a black dashed line. We compute the synthetic data using a top layer velocity of $v_p = 2500$ m.s^{-1}, and we use the true velocity in the half-space for the sake of this illustration. We show the synthetic trace in a red solid line. The extended calculated trace is extracted from the synthetic wavefield (shown in gray scale in Figure 1d) at the moving receiver positions (white solid line). Moving the receiver following this relocalization time profile, allows to fit both arrivals. The extended trace is shown in a blue solid line. We aim in this study at substituting this parametrization and the subsequent optimization, with a dynamic programming strategy.

On the analogy between dynamic time warping and receiver extension

In the study of Ma and Hale (2013), dynamic programming was used in wave equation tomography, which is formulated as

$$\min_{\tau} f_{\mathbf{T}} = \min_{\tau} \frac{1}{2} \sum_{s=1}^{N_s} \sum_{r=1}^{N_r} \int \tau_{s,r}(t)^2 dt, \tag{4}$$

where $\tau_{s,r}(t)$ is a time-varying time shift. The latter is obtained through the following constrained minimization

$$\tau_{s,r} = \underset{l}{\text{argmin}}\ D_{s,r}(l), \text{ subject to } \left| \frac{\partial \tau_{s,r}}{\partial t} \right| \leq \sigma_t, \tag{5}$$

where $D_{s,r}(l)$ is defined as

$$D_{s,r}(l) = \int |d_{cal,s}(\mathbf{x}_r, t + l_r(t)) - d_{obs,s}(\mathbf{x}_r, t)|^2 dt, \tag{6}$$

where l is a time-varying time-shift. The constraint in equation 5 controls the amount of time-shift from one time sample to the next. Interestingly enough, the reconstruction of the time varying time shift $\tau_{s,r}(t)$ is very close to our inner loop problem. Looking at equations 1 and 6, one can observe that in the DTW case, a time-dependent time-shift $\tau_{s,r}(t)$ is sought for each synthetic trace so as to minimize the least-squares distance between observed and calculated data. In our time-dependent receiver extension case, we do the same, except that a time-dependent receiver spatial shift is sought for each trace instead of a time-dependent time-shift. Of note, this difference implies that in our case, the extended calculated data always satisfy the wave equation, which is not the case for DTW. This analogy also makes it possible to use dynamic programming to compute the time-dependent receiver extension $\Delta x_{s,r}(t)$ directly, without going through a polynomial parametrization. We thus formulate our inner loop as

$$\overline{\Delta x_{s,r}(t)} = \underset{\Delta x(t)}{\text{argmin}} f(m, \Delta x(t)), \quad \text{subject to } \left| \frac{\partial \overline{\Delta x_{s,r}(t)}}{\partial t} \right| \leq \sigma_x. \tag{7}$$

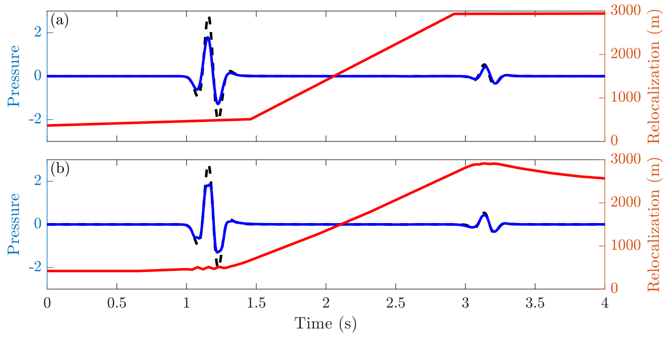

Figure 2: *Time-dependent receiver extension illustration using (a): polynomial parametrization with PSO, and (b): dynamic programming. The observed trave is shown in a black dashed line, and the extended synthetic in a solid blue line. The relocalization time profiles are shown in red solid lines.*

The constraint in equation 7 controls the receiver speed. Similar to DTW, receiver extension can be solved using dynamic programming because it can be broken down into smaller and nested sub problems. That is, if a relocalization time profile is optimal, then a portion of it is also optimal (Bellman principle of optimality (Kirk, 1970)). We illustrate our new approach using the previous example from Figure 1: we show the data fit, as well as the relocalization profile obtained using both the dynamic programming and the polynomial approaches in Figure 2. The fit for both arrivals is obtained using both approaches, and the relocalization profiles are very similar. We note that for our polynomial parametrization, the number of segments as well as the order of polynomials need to be defined a priori. In this example, the number of degrees of freedom is 4 (three segments with first order Lagrange polynomials). Solving this problem with stochastic optimization (PSO in this example) requires tuning: defining the number iterations and various parameters (number of particles, boundary conditions, and other parameters specific to PSO). The dynamic programming approach does not rely on the polynomial parametrization: the number of unknowns is simply equal to the number of time samples of the seismic traces. In addition, this optimization strategy is deterministic, and controlled by less tuning parameters. As for the computational cost, the dynamic programming approach is considerably cheaper. The dynamic programming problem of equation 7 is solved in three steps: computation of pointwise misfit function (time sample by time sample), summation of the misfit following permissible paths, which honor the constraint in equation 7, and finally, a recursion to reconstruct the solution. The interested reader is referred to Hale (2013).

FWI example: a North Sea exploration scale 2D synthetic model

We test our method using a synthetic North Sea exploration scale synthetic model. We generate the observed data using the true model under the acoustic approximation. The initial model is obtained by a Gaussian smoothing of the true model. First, we perform 300 iterations of conventional FWI. As expected, it is unable to reconstruct the velocity model, starting from this crude initial model.

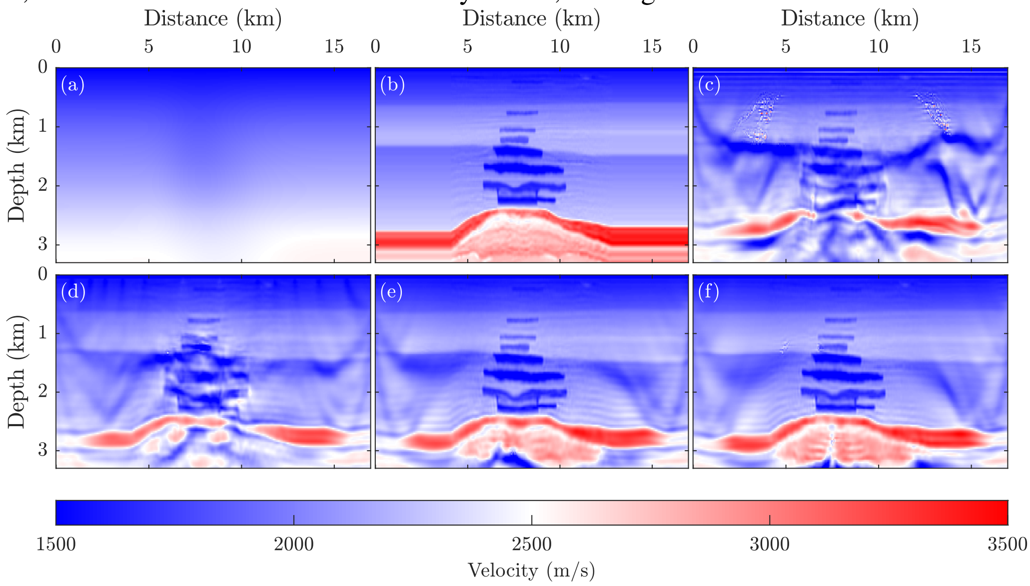

Figure 3: *Numerical example using a North Sea 2D synthetic model, 300 iterations are performed for all tests. (a): Initial velocity model, (b): true velocity model, (c): reconstructed model using conventional FWI, (d): reconstructed model using static receiver extension, (e): reconstructed model using time-dependent receiver extension with PSO for the inner loop, and (f): reconstructed model using time-dependent receiver extension with dynamic programming.*

Then we compare three receiver extension strategies: first, we perform 300 iterations of static receiver extension (Métivier and Brossier, 2022), then, 300 iterations of time-dependent receiver extension with polynomial parametrization and stochastic optimization (Benziane et al., 2024), and finally, 300 iteration of time-dependent receiver extension with dynamic programming. Static receiver extension performs better than conventional FWI, however, the reconstructed model contains clearly visible cycle-skipping artifacts. The reconstruction may be improved with more iterations. Time-dependent receiver extension with polynomial parametrization is able to fully reconstruct the low velocity anomaly in the center of the model, as well as most of the high velocity basement. As for the dynamic programming approach, the reconstructed model is of the same quality (compared to the one obtained using the polynomial parametrization). We note however that the lower part of the high velocity basement is better resolved with our new approach.

These results are encouraging, because the reconstruction is satisfactory. In addition, the cost of the dynamic programming approach is significantly lower. We show the CPU time required to perform the different steps of computation in Table 1. The CPU times for forward simulation, inner loop computation as well as the adjoint simulation and gradient summation are shown for conventional FWI, static receiver extension, time-dependent receiver extension with PSO and time-dependent receiver extension with dynamic programming. The computational overhead for the static approach is negligible, which is not the case for the time-dependent strategy with PSO. The dynamic programming approach provides comparable results, with less computational burden. Please note the slight increase in the adjoint simulation CPU time, it is attributed it to the adjoint source injection at time-dependent receiver positions, which is performed at all time steps.

	Forward simulation	Inner loop	Inner loop per receiver	Adjoint simulation+ gradient summation
Conventional FWI	13.24	-	-	38.88
Static	13.26	2.94	1.73×10^{-2}	39.27
Time-dependent (PSO)	13.18	55.6	0.32	43.70
Time-dependent (DP)	13.21	10.16	6.15×10^{-2}	41.92

Table 1: *CPU times in seconds for the different steps of the computation.*

Conclusion and perspectives

We have developed an alternative method to solve the inner loop problem using a dynamic programming approach, similar to dynamic time warping of seismic images (DTW). This new strategy provides satisfactory model reconstructions, starting from a crude intial model. It also eliminates the need to use stochastic optimization, which is more costly and inherently non-repeatable. This method is particularly interesting for large scale 3D FWI, where the number of receivers is large.

Acknowledgements

This study was partially funded by the SEISCOPE consortium (*http://seiscope2.osug.fr*), sponsored by AKERBP, DUG, EXXONMOBIL, GEOLINKS, JGI, PETROBRAS, SHELL, SINOPEC, TOTALENERGIES and VIRIDIEN. This study was granted access to the HPC resources provided by the GRICAD infrastructure (https://gricad.univ-grenoble-alpes.fr), which is supported by Grenoble research communities, the HPC resources of Cray Marketing Partner Network (`https://partners.cray.com`), and those of CINES/IDRIS/TGCC under the allocation 046091 made by GENCI.

References

Benziane, M., Brossier, R., Métivier, L. and Sambolian, S. [2024] Full-waveform inversion with time-dependent receiver-extension: An efficient inner loop optimization. In: *Fourth International Meeting for Applied Geoscience & Energy*. 1038–1042.

Hale, D. [2013] Dynamic warping of seismic images. *Geophysics*, **78**(2), S105–S115.

Kennedy, J. and Eberhart, R. [1995] Particle swarm optimization. In: *Proceedings of ICNN'95 - International Conference on Neural Networks*, 4. 1942–1948 vol.4.

Kirk, D.E. [1970] *Optimal control theory : an introduction / Donald E. Kirk,...* Prentice-Hall networks series. Prentice-Hall, Englewood Cliffs, N.J.

Ma, Y. and Hale, D. [2013] Wave-equation reflection traveltime inversion with dynamic warping and full waveform inversion. *Geophysics*, **78**(6), R223–R233.

Métivier, L. and Brossier, R. [2022] Receiver-extension strategy for time-domain full-waveform inversion using a relocalization approach. *Geophysics*, **87**(1), R13–R33.

Virieux, J. and Operto, S. [2009] An overview of full waveform inversion in exploration geophysics. *Geophysics*, **74**(6), WCC1–WCC26.